The non-conservative distribution pattern of organic matter in Rajang, a tropical river with peatland in its estuary

Zhuo-Yi Zhu[1]*, Joanne Oakes[2], Bradley Eyre[2], You-You Hao[1], Edwin Sien Aun Sia[3], Shan Jiang[1], Moritz Müller[3], Jing Zhang[1]

1. State Key Laboratory of Estuarine and Coastal Research, East China Normal University, Shanghai, 200241, China

2. Centre for Coastal Biogeochemistry, School of Environment, Science and Engineering, Southern Cross University, Lismore NSW, 2480, Australia

3. Swinburne University of Technology, Faculty of Engineering, Computing and Science, Jalan Simpang Tiga, Kuching, 93350, Sarawak, Malaysia

*Corresponding author: Z.Y. Zhu, zyzhu@sklec.ecnu.edu.cn; zhu.zhuoyi@163.com

Abstract

South-east Asian peatland-draining rivers have attracted much attention due to their high dissolved organic carbon (DOC) yield and high CO_2 emissions under anthropogenic activities. In August 2016, we carried out a field investigation of the Rajang river and estuary, a tropical system located in Sarawak, Malaysia. The Rajang has peatland in its estuary while the river basin is covered by tropical rainforest. DOC $\delta^{13}C$ in the Rajang ranged from -28.7‰ to -20.1‰ and a U-shaped trend from river to estuary was identified. For particulate organic carbon (POC), the $\delta^{13}C$ ranged between –29.4‰ to –31.1‰ in the river and a clear increasing trend towards more $\delta^{13}C$ -enriched with higher salinity existed in the estuary. In the estuary, there was a linear conservative dilution pattern for dissolved organic matter composition (as quantified by D/L amino acids enantiomers) plotted against DOC $\delta^{13}C$, whereas when plotted against salinity dissolved D/L amino acids enantiomers values were higher than the theoretical dilution value. Together, these data indicate that the addition of DOC in estuary (by peatland) not only increased the DOC concentration, but also altered its composition, by adding more bio-degraded, ^{13}C-depleted organic matter into the bulk dissolved organic matter. Alteration of organic matter composition (adding of more degraded subpart) was also apparent for the particulate phase, but patterns were less clear. The Rajang was characterized by DOC/DON ratios of 50 in the river section, with loss of DON in the estuary increased the ratio to 140, suggesting the unbalanced export pattern for organic carbon and nitrogen, respectively. Under anthropogenic activities, further assessment of organic carbon to nitrogen ratio is needed.

Keyword

Amino acids enantiomers, DOC, POC, stable carbon isotope, Rajang, peatland

1. Introduction

Fluxes and cycling of organic matter (OM) in rivers and estuaries are important influences on global biogeochemical cycles and climate change. In river basins, vascular plants are the ultimate sources of organic matter (Hedges and Man, 1979), but algae, moss and bacteria are also important (Hernes et al., 2007). As well as providing a source of OM, bacteria may also strongly modify the composition of organic matter within a river and its resistance to degradation. The lability of organic matter determines how rapidly organic carbon will be transformed into inorganic carbon (CO_2), which can vary from hours to millions of years. The lability of organic matter therefore plays a role in determining whether organic matter is either a source or a sink of carbon in the atmosphere (Zhang et al., 2018). Based on ^{14}C of organic carbon, Mayorga et al. (2005) determined that the degradation of recently synthesized organic matter in the river basin was the main reason Amazonian river waters were supersaturated in CO_2, and hence the a source of atmospheric CO_2. This highlights the potential importance of organic matter stability for carbon cycling within river systems. Nitrogen is another important element in organic matter, which is not independent from carbon, but instead is closely combined with carbon in various chemical compounds (like amino acids). Due to the nature of these specific compounds, the behavior of bulk carbon and nitrogen can differ substantially. In basins with peatland, the leaching of DOC is related to the status of peatland (disturbed vs undisturbed), whereas the leaching of dissolved organic nitrogen (DON) is controlled by the soil inorganic nitrogen content (Kalbitz and Geyer, 2002). The different leaching mechanisms of organic carbon and nitrogen indicates that the comparison of these two elements would deepen our understanding of organic matter cycles.

Tropical south-east Asian rivers play an important role in both dissolved and particulate organic

58   matter export (Baum et al., 2007; Huang et al., 2017; Müller et al., 2016). Located in Sarawak,

59   Malaysia (Fig. 1a), the turbid Rajang river (hereafter refer to as the Rajang) is the longest river in

60   Malaysia. The Rajang flows through tropical rainforest, and peatland and mangroves are distributed

61   in the estuary. A dam was constructed in the upper reaches of the Rajang in 2015, but the total

62   suspended matter (TSM) in the river remains at 100 – 200 mg/L in recent years (Müller-Dum et al.,

63   2019). Dilution of terrestrial organic matter in the adjacent coast is expected, while turbid river

64   water strongly limits apparent organic matter photo-degradation within the river and estuary, leaving

65   the stage of fluvial organic matter alteration to bacteria utilization and abiotic process like

66   desorption/adsorption between particulate and dissolved phase (Martin et al., 2018). Further,

67   dissolved oxygen is negatively related to pCO_2, likely due to in-stream heterotrophic respiration

68   (Müller-Dum et al., 2019). In the Rajang brackish estuary, where peatland is located, addition of

69   peatland DOC into river water is suggested by the non-conservative mixing pattern of DOC with

70   increasing salinity (Martin et al., 2018), whereas removal of DON in the Rajang estuary is suggested

71   by nitrogen stable isotopes (Jiang et al., 2019).

72   While stable isotopes of carbon and nitrogen are useful tools for tracing organic matter, amino

73   acids (AAs) are the most important organic carbon and nitrogen carriers that have been chemically

74   identified, accounting for up to ~100% of the particulate nitrogen in aquatic environments, and up

75   to nearly half of the particulate organic carbon pool (Jennerjahn et al., 2004). Due to the selective

76   removal and accumulation of certain amino acids, amino acids are important biomarkers in early

77   diagenesis, allowing quantification of organic matter lability/resistance (Dauwe and Middelburg,

78   1998; Kaiser and Benner, 2009). With the exception of glycine, amino acids are chiral. L forms of

79   amino acids are from animals, plants and plankton, whereas D forms mainly come from bacteria,

80   and are key chemical compounds in peptidoglycan, which forms the basic structure of bacterial cell

81   membranes (Vollmer et al., 2008). Due to the key role of bacteria in OM alteration and early

82   diagenesis, D-AAs (D forms AAs) tend to accumulate during OM degradation. A higher ratio of D-

83   to L-AAs (D/L ratio) therefore indicates more that OM is more refractory (Davis et al., 2009). As a

84   non-protein amino acid, accumulation of GABA (γ－aminobutyric acid) is also highly related to

85   OM degradation (Davis et al., 2009). Conversely, a lower D/L ratio and GABA% indicates that OM

86   is relatively less degraded, and hence more labile. In river waters, elevated D-AAs also indicates

87   the presence of soil humic substances, which is a product of bacteria and their detritus (Kimber et

88   al., 1990).

89   Tropical rivers are dominated by refractory (or bio-degraded) organic matter, yet labile OM is

90   also known to play a role in river carbon cycles (Mayorga et al., 2005). It is hence expected that the

91   fluvial organic matter in the river would be a mixture of labile organic matter (that can be respired

92   to support pCO_2) and refractory terrestrial organic matter (that will be diluted/degraded after

93   entering the sea (Martin et al., 2018), while in the estuary there would be addition of dissolved OM

94   from peatland/mangrove (Dittmar et al., 2001b; Müller et al., 2016). Previous studies of OM in

95   south-east Asian rivers mainly focused on its bulk concentrations, ages, or optical properties (Martin

96   et al., 2018 and ref. therein). The use of biomarker approaches has been very limited (Baum et al.,

97   2007; Gandois et al., 2014). Given the processes described above and their potential contribution to

98   the carbon (Müller-Dum et al., 2019) and nitrogen cycles (Jiang et al., 2019), it is somewhat

99   surprising that there has been limited application of amino acid approaches, including D-AAs, to

100   investigate organic matter composition and the role of estuarine peatland/mangrove in OM

101   regulation (Jennerjahn et al., 2004). South-east Asian rivers are subject to multiple stressors due to

102 increasing anthropogenic activities in both their riverine (e.g., damming, logging/secondary

103 plantation) and estuarine sections (e.g., drainage, and oil palm plantations) (Hooijer et al., 2015).

104 AAs enantiomers and carbon/nitrogen isotopes have the ability to provide molecular level evidence

105 for the impact of these stressors on carbon and nitrogen cycling and bulk biogeochemistry, as well

106 as insight into the mechanisms underlying such changes.

107   In this study, we carried out a field investigation in the Rajang in August 2016, from S10 to S1

108 station, located on the coast of the South China Sea adjacent to the Rajang (Fig. 1b). AAs

109 enantiomers and $\delta^{13}C$ of DOC were used to elucidate the succession of organic matter

110 sources/composition from the fresh water to the estuarine sections of the Rajang. Our aim was to

111 address the following questions: 1) Given that peatland contributes additional DOC to fluvial DOC

112 (Müller et al., 2016), does the composition of dissolved OM change from river to estuary? 2) Do

113 changes in organic nitrogen mirror changes in organic carbon? 3) And hence what is the role of

114 peatland/mangroves on OM composition and lability in the Rajang? Globally, rivers in low latitudes

115 receive much less attention relative to temperate and polar rivers (36 vs. 958 studies)(Cloern et al.,

116 2014), while they could equally important in carbon cycle (Cloern et al., 2014). Our work, together

117 with other tropical studies, would enrich the understandings for organic carbon and nitrogen cycles

118 in tropical rivers/estuaries.

119

120 **2. Materials and methods**

121   All abbreviations, together with the amino acids measured in this study, are listed in table 1.

122 **2.1 Brief background**

123   The Rajang river and estuary is located in Sarawak, Malaysia. The climate is wet year-round,

124   but the main precipitation typically occurs in winter (November to February). Climate is influenced

125   by El Niño-Southern Oscillation (ENSO) and Madden-Julian Oscillation. In August 2016, the

126   discharge was estimated as 2440 m^3/s, in comparison with an annual mean discharge of 4000 m^3/s

127   for 2016 and 2017 (Müller-Dum et al., 2019).

128   Based on salinity, station S5 is regarded as the boundary of the fresh and estuarine water of the

129   Rajang (Fig. 1b). In this work all samples with a salinity of 0 were regarded as fresh water, while

130   samples with salinity >0 were regarded as estuarine. In the estuary, there are several branches,

131   namely Igan, Lassa, Paloh, and Rajang itself (Fig. 1b). Since water in all these branches are from

132   Rajang river (i.e., upstream of S5), in this work all these branches are regarded as the Rajang estuary.

133   Peatland and mangroves are commonly distributed in the estuary (shown in Fig. 1b) while tropical

134   rainforest is widely distributed upstream of S5 (not shown in Fig. 1b). The peatland is under strong

135   pressure of draining and change of use for oil palm, while in the basin logging and secondary growth

136   is very common (Hooijer et al., 2015). Compared with other peatland-draining tropical blackwater

137   rivers, the Rajang is more like a turbid tropical rainforest river (Müller-Dum et al., 2019), but with

138   notable peatland/mangrove in its estuary (Fig. 1b).

139   **2.2 Field sampling**

140   The field work was carried out in August 2016. The sampling stations covered from S10 (the

141   upper most station in this study) to S1 on the coast. At each station, a pre-cleaned and sample-rinsed

142   bucket was used to collect surface water from the center of the channel in a boat. After sample

143   collection, pretreatment was done immediately on board in the boat. For DOC and its stable carbon

144   isotope ratios (δ^{13}C), water samples were collected by syringe filtering (pre-combusted Whatman

145   GF/F; 0.7 μm) approximately 30 ml of sample water into a pre-combusted 40 ml borosilicate vial.

146 Samples were preserved with five drops of concentrated phosphoric acid and sealed with a lid

147 containing a Teflon-coated septa. For total dissolved amino acids (TDAA), water samples were

148 filtered through a 0.4 μm nylon filter. For particulate OM samples (TSM, POC, POC-δ^{13}C, PN and

149 PN-δ^{15}N, and total particulate amino acids (TPAA)), suspended particles were concentrated onto

150 glass fiber membrane (pre-combusted Whatman GF/F; 0.7 μm). The GF/F filters were folded and

151 packed in pre-combusted aluminum. All samples were immediately stored frozen (–20°C) until

152 analysis. At every station both particulate and dissolved samples were collected, but a few samples

153 were broken/missing during transportation back to Shanghai. This includes the particulate (POC

154 and TSM) samples at station S16 (conductivity = 64 μS/cm), station S4 (salinity = 4.8), station S25

155 (salinity = 11.7) and at station S29 (salinity = 4.3) and a dissolved (TDAA) sample at station S24

156 (salinity = 19.1). A portable meter (Aquaread, AP-2000) was used to obtain conductivity/salinity,

157 temperature, dissolved oxygen and pH.

158 **2.3 Laboratory analyses**

159 Concentrations and δ^{13}C of DOC were measured via continuous-flow wet oxidation isotope-

160 ratio mass spectrometry using an Aurora 1030W total organic carbon analyzer coupled to a Thermo

161 Delta V IRMS (Oakes et al. 2010). Glucose of known isotopic composition dissolved in He-purged

162 Milli-Q was used as a standard to correct for drift and to verify sample concentrations and δ^{13}C

163 values. Reproducibility for concentrations and δ^{13}C was ± 0.2 mg l^{-1} and ± 0.4 ‰. DOC

164 concentrations and δ^{13}C were measured at the Centre for Coastal Biogeochemistry at Southern Cross

165 University (Lismore, Australia). For the determination of POC, samples (GF/F glass fiber filter)

166 were freeze-dried and analyzed with a CHNOS analyzer (Model: Vario EL III) after removing the

167 inorganic carbon by reaction with HCl vapor. For PN, a similar procedure like that of POC was used,

168 but no acid was used in pre-treatment. The detection limit for POC was 7.5×10^{-6} g, with precision

169 better than 6%, based on repeated determinations (Zhu et al., 2006). The POC-δ^{13}C and PN-δ^{15}N

170 were determined using a DELTA^{plus}/XL isotopic ratio mass spectrometer (Finnigan MAT Com. USA)

171 interfaced with a Carlo Erba 2500 elemental analyzer. The standard for δ^{13}C was PDB and the

172 precision of the analysis was ± 0.2‰. For δ^{15}N, the standard was air and precision was ± 0.3‰.

173 Total hydrolyzable AAs were extracted and analyzed following the method of Fitznar et al., (1999)

174 with slight modifications (Zhu et al., 2014). Briefly, samples were first hydrolyzed with HCl at

175 110°C. After pre-column derivatization with o-Phthaldialdehyde (OPA) and N-Isobutyryl-L/D-

176 cysteine (IBLC/IBDC), AAs and their enantiomers were analyzed using an HPLC (Agilent 1200)

177 comprising of an online vacuum degasser, a quaternary pump, an auto-sampler, a thermostatted

178 column and a fluorescence detector (excitation 330 nm, emission 445 nm). The analytical column

179 was a Phenomenex Hyperclone column (BDS C18, 250×4mm, 5μm) with a corresponding pre-

180 column. To eliminate the influence of racemization of L-type AAs in the hydrolysis process, the

181 concentration of D/L AAs measured in actual samples was corrected according to the formula

182 obtained by Kaiser and Benner (2005). The detection limit for glycine (Gly) and individual AAs

183 enantiomers were in the lower picomolar level. Asx and Glx were used for aspartic acid + asparagine

184 and glutamic acid + glutamine, respectively (Table 1), as the corresponding acids are formed via

185 deamination during hydrolysis.

186 A few samples (e.g., TDAA in S1 station) were not measured due to instrument hardware problem.

187 And hence the measured particulate and dissolved sample stations did not exactly match.

188

189 **3. Results**

190   In August 2016, the TSM concentration in the Rajang ranged from 22 mg/L (mean for the fresh

191 water section: 61 mg/L) to 161 mg/L (mean for the estuarine section: 73 mg/L) (Table 2).

192 Throughout the system DOC concentrations exceeded POC concentrations. DOC and POC in the

193 fresh water section averaged 337 μM and 86 μM, and in the estuarine section 345 μM and 64 μM,

194 respectively (Table 2). While DOC concentration was slightly higher in the estuary than in the fresh

195 water (Table 2), a maximum of both DOC and POC can be found at around salinity 15 to 20 in the

196 estuary (Fig. 2).

197   DOC $\delta^{13}C$ ranged from −28.7‰ to −20.1‰ (Table 2). A U-shaped trend from fresh water

198 section to estuary section can be identified for DOC $\delta^{13}C$, with one outlier from the Rajang main

199 stream at a salinity of 5 (S2 station; Fig. 3a). The minimum value of DOC $\delta^{13}C$ (bottom of the U)

200 was detected at a salinity of ~10 (Fig. 3a). For particulate OM, $\delta^{13}C$ ranged between −29.4‰ to −

201 31.1‰ in the fresh water section. In the estuary section, there was a clear increasing trend with

202 increasing salinity, from −30‰ (S=1.1) to values close to −24‰ (S>30) (Fig. 3b).

203   In the fresh water section, the mean TDAA and TPAA concentrations were 0.3 μM and 2.5

204 μM, respectively (Table 3). For TDAA, the AA carbon yield (the carbon from AA divided by bulk

205 DOC or POC, in %) in both fresh water and estuary sections were very similar, namely 0.40% and

206 0.38% (mean), respectively (Table 3), whereas AA nitrogen yield was higher in the estuary (11%)

207 than in the fresh water section (4.8%) (Table 3). For TPAA, there was little difference between the

208 fresh water and estuary sections in AA carbon yield (13.5% and 16.8%, respectively) and nitrogen

209 yield (66% and 62%, respectively) (Table 3).

210   With respect to individual AA compounds, in both dissolved and particulate phase, Gly, Glx,

211 Ala and Asx were the most abundant AAs. These four AAs together accounted for 66% of TDAA

and 47% of TPAA in the fresh water section, 59% of TDAA and 48% of TPAA in the estuary. The

non-protein AA GABA was detected in trace amounts, but was accumulated in the dissolved phase

relative to the particulate phase, as indicated by the higher GABA% in the dissolved phase (Table

3). GABA% decreased from 2% (fresh water section mean) to 1.3% (estuarine section mean) in the

dissolved phase, and decreased from 0.7% (fresh water section mean) to 0.4% (estuarine section

mean) in the particulate phase (Table 3). In the estuary, GABA% in the dissolved phase remained

stable (~1.5%) in brackish water (salinity 5 to 20) and quickly dropped to <1% where salinity was

over 30 (Fig. 4a). Most of the GABA% data dots were above the theoretical mixing line (Fig. 4a).

In the particulate phase, there was an overall decrease in GABA% with increasing salinity within

the estuary (Fig. 4b).

As for the AA enantiomers, the percentage of D- form AA in TDAA averaged 12% for both

fresh water and estuarine section. The most abundant D-form AAs in the dissolved phase were Glx

and Asx. For the particulate phase, percentage of D- form AA in TPAA was much lower relative to

that in dissolved form, decreasing from a mean of 4.4% in the fresh water section to a mean of 3.3%

in the estuary (Table 3). And patterns in the variation of D/L Glx (Fig. 5) along with

conductivity/salinity gradient in the Rajang were similar to those for GABA% (Fig. 4) for both

dissolved and particulate phase. For example, for dissolved phase, the pattern of decreasing D/L

ratio along with increasing salinity was nearly absent (Fig. 5a), whereas for particulate phase such

decreasing pattern was much clearer in the estuary (Fig. 5b). Similar to GABA%, all the dissolved

samples showed elevated values (i.e., dots above the theoretical dilution line) for D/L Glx in the

estuary (Figs. 4a and 5a).

4. Discussion

4.1 Distribution patterns of OM composition

Dissolved OM

Terrestrial OM usually has a more negative $\delta^{13}C$ value (–32‰ to –26‰ for C3 plants), whereas marine OM has more positive value values ($\delta^{13}C$, ~ –20‰)(Lamb et al., 2006; Mayorga et al., 2005). Overall, the very negative $\delta^{13}C$ values for DOC (<–26‰) in the river part of the Rajang indicates that the OM had a very clear C3 plant source (e.g., mangroves and oil palms (Jennerjahn et al., 2004; Lamade et al., 2009; Wu et al., 2019)), whereas DOC $\delta^{13}C$ values > –24‰ in the estuary (salinity >30) suggests a mixture of terrestrial and marine OM (Fig. 3a). The most depleted $\delta^{13}C$ values for DOC occurred at a salinity of 10 (Fig. 3a). Above this salinity, the influence of marine OM became more overwhelming, and the bulk DOC $\delta^{13}C$ signal was more enriched (Fig. 3a).

Among samples in the fresh water section, the sample of most enriched DOC-$\delta^{13}C$ value (S10 and S15; DOC-$\delta^{13}C$: –25‰; Fig. 3a) although initially appearing to be outliers, were characterized by very elevated D/L amino acids ratios (Fig. 6a). This was particularly the case for the sample from S10 (the upper most station in this study; Fig. 1b), which showed a maximum D/L Glx ratio of 0.57 (Fig. 6a). In addition, these samples from S10 and S15 also showed a higher D/L ratio for Asp (S10: 0.49, S15: 0.38; figure not shown) when compared to all fresh water or estuary samples (mean: 0.34; Table 3). On land, D form amino acids can be derived from abiotic racemization process (which requires a very long time scale) in which L form amino acids slowly changes into their corresponding D form (Schroeder and Bada, 1976). More significantly in contemporary environments, D form amino acids are widely synthesized by bacteria during their cell membrane construction (Schleifer and Kandler, 1972). D/L Glutamic acid and D/L Aspartic acid ratios of pure

256   peptidoglycan (*Staphylococcus aureus*, Gram-positive) are 0.49 and 0.30, respectively (Amon et al.,

257   2001). Though $\delta^{13}C$ values for bacteria in the Rajang remains unclear, bacteria have been reported

258   to have $\delta^{13}C$ values from –12‰ to –27‰ (Lamb et al., 2006). Contribution of OM derived from

259   bacteria may therefore explain the relatively enriched $\delta^{13}C$ values observed at inland S10 station

260   and S15. A possible OM source at these stations is soil humic substances, which is expected to be

261   under strong impact of bacteria, and has a high contribution of D-form amino acids (Dittmar et al.,

262   2001a). A more depleted pattern of DOC $\delta^{13}C$ from mountain to lowland is suggested to be due to

263   dilution and mixing with younger OM in the lowland (Mayorga et al., 2005). This is consistent with

264   our findings that, depleted pattern of riverine DOC $\delta^{13}C$ within the fresh water section was

265   corresponding to a lowering D/L ratio pattern, which indicates the dilution with less degraded OM

266   (see orange circles in Fig. 6a). Whether the dissolved samples with elevated D/L ratio and relatively

267   positive $\delta^{13}C$ in the fresh water section (S10 and S15; Fig. 6a) reflect the presence of soil humic

268   substances, or instead reflect the direct presence of bacteria, requires further study.

269   In the estuarine section, it was very clear that terrestrial bio-degraded OM (indicated by

270   elevated D/L ratios and more negative $\delta^{13}C$) is diluted with more labile OM (lower in D/L ratio but

271   more positive $\delta^{13}C$)(see blue solid dots in Fig. 6a). However, this apparent dilution trend became

272   very vague (or showed no trend) when D/L ratio was plotted against salinity (Fig. 5a). This was also

273   confirmed by the GABA% distribution pattern which showed a platform-like pattern at a salinity

274   between 5 and 20 (Fig. 4a). Though TDAA at S1 is missing, the composition of TDAA at S2

275   (salinity = 31.2) was very typical of marine OM (i.e., very low D/L ratio and relatively enriched

276   DOC-$\delta^{13}C$; see Fig. 6a). Hence in the estuary there is a conservative distribution pattern for

277   dissolved OM when plotted against $\delta^{13}C$ (Fig. 6a) but such pattern disappeared when plotted against

salinity (Figs. 4a&5a). The location above the conservative dilution line of all OM data in the

brackish estuary (salinity between 10 and 25; Figs. 4a&5a), indicates that the OM in the estuarine

section was more degraded than theoretically expected. The combination of degraded OM with the

observed DOC concentration increase in the estuary (345 μM in the estuary vs. 337 μM in the fresh

water section; or Fig. 2b), suggests the addition of degraded DOC to the Rajang. Non-conservative

dissolved OM behavior in the estuary has previously been reported based on an optical approach

(Martin et al., 2018), and minimal OM alteration during estuarine transport was suggested (Martin

et al., 2018). Hence, it is reasonable that changes in dissolved OM composition (Figs. 4a&5a) may

largely take place in land/estuary (e.g., in pore waters of soil) and impact the Rajang riverine

dissolved OM via leaching from soils.

Particulate OM

As for particulate OM, depleted POC-δ^{13}C in the river part of the Rajang indicated the strong

influence of terrestrial OM (e.g., C3 plant; Dittmar et al., 2001b) whereas in the estuary, particulate

OM was diluted with marine particulate OM, as indicated by the seawards enrichment of δ^{13}C (Fig.

3b). In the sediment, a clear woody angiosperm C3 plants as the OM source is found based on a

lignin approach (Wu et al., 2019), and similar increases in carbon and nitrogen isotopes in suspended

particles in brackish water have also been observed in other estuaries (Cifuentes et al., 1996;

Raymond and Bauer, 2001). Unlike dissolved OM, there were no samples with unusually enriched

δ^{13}C values in the fresh water section (Figs. 6b&c). D/L Glx ratio in the fresh water section is higher

when compared with that in the estuary section (Table 3), and overall, when compared with

dissolved OM, particulate OM basically became more labile when transporting seawards, as

indicated by its composition shift along with salinity (Figs. 4b&5b) or isotope (Figs. 6b&c).

300   Although particulate OM had a lower D/L ratio than dissolved OM (Fig. 6), it should be noted

301   that this does not mean dissolved OM is more aged or degraded than particulate OM. Riverine POM

302   and DOM usually show different ages (Bianchi and Bauer, 2011), while selective

303   desorption/adsorption of bacteria and related detritus between particulate and dissolved phase also

304   strongly modifies the biomarker-indicated degradation status of OM (Dittmar et al., 2001a).

305   **4.2 Different fate of bulk organic carbon and nitrogen**

306   Leaching of DOC and DON from peatlands is driven by difference mechanisms: DOC release

307   is related to the status of peatland (pristine vs. degraded), whereas DON release is determined by

308   the DIN content of peatland soil (Kalbitz and Geyer, 2002). In the Rajang, bulk DOC and DON

309   concentrations were not coupled, as suggested by the DOC/DON ratio variation pattern (Fig. 7).

310   The average DOC concentration in the estuary part was slightly higher (345 μM) than in the river

311   part (337 μM; Table 3), which indicates the addition of DOC in the estuary. In comparison, the

312   removal of DON in the estuary is suggested (Jiang et al., 2019).

313   In the Rajang, non-conservative dilution behavior from optical properties was observed for

314   estuarine DOC (Martin et al., 2018), which is consistent with other peatland-draining rivers in

315   Sarawak (Müller et al., 2016). The contribution of marine sources to dissolved OM is reflected in

316   the increasing DOC-δ^{13}C in the estuary part (Fig. 3a). Peatland, however, is known for its high

317   contribution to fluvial DOC and has been suggested to contribute to the DOC in the Rajang (Martin

318   et al., 2018). In peatland-draining rivers west of the Rajang, the DOC concentration endmember can

319   be as high as 3690 μM (Müller et al., 2015). Under such high DOC background, a simple three-

320   endmember mixing model (i.e., a model that based on the endmembers of first observed fresh water

321   DOC endmember, second peatland DOC endmember and third a calculated fresh water DOC

endmember) suggested that peatland-DOC addition accounts for 3% of the fluvial DOC in the Saribas river and 15% in the Lupar river (Müller et al., 2016). Assuming that peatland in the Rajang estuary has a comparable endmember DOC concentration to other peatland in Sarawak (i.e., 3690 μM; Müller et al., 2015), and given our observed Rajang fresh water DOC endmember value of 337 μM (DOC concentration at S5 station) and a marine DOC endmember of 238 μM (S1 station), a similar model approach suggests peatland DOC addition contributed 4% of the Rajang fluvial DOC, which is comparable to Saribas river and much lower than Lupar river (Müller et al., 2016). In the meantime, as mentioned in the previous section, there is a non-conservative dilution pattern, with dissolved OM in the estuary part more degraded than expected based on simple dilution with a marine endmember (Figs. 4a&5a). Hence it is reasonable that peatland not only contributed to the fluvial DOC in concentration (Martin et al., 2018), but also modified the dissolved OM composition (more bio-degraded) in the estuary. In another tropical river study, mangrove in the estuary exerted a stronger influence on fluvial dissolved OM than hinterland vegetation (Dittmar et al., 2001b). This is consistent with the Rajang, for which estuarine processes apparently impact the dissolved OM in terms of both DOC concentration (by increasing the bulk amount) and composition (by adding bio-degraded DOC). The estuarine dissolved OM showed higher bio-degraded feature (e.g., elevated GABA% and D/L ratio; Figs. 4a&5a), but this subpart may be photolabile (Martin et al., 2018). When TSM decreases and light condition in the water column becomes good (e.g., entering the sea), photodegradation is expected (Martin et al., 2018). Other oceanic degradation mechanisms include the priming effect (Bianchi, 2011). The fate of the terrestrial OM in the sea requires further study. As we lack the DON concentration endmember in peatland, peatland impact on DON in the estuary is not estimated.

344   In contrast to DOC, which was apparently added to the estuary, DON was removed,

345   contributing to a remarkable increase of dissolved inorganic nitrogen in the estuary (Jiang et al.,

346   2019). In the fresh water section, the nitrate concentration was not related to the ratio of D/L

347   dissolved AAs, nor related to dissolved GABA% (Fig. 8), and in the estuarine section, nitrate was

348   not related to D/L AAs but it indeed was related to GABA% in the estuarine section (Fig. 8b). This

349   indicates that fluvial nitrate in the fresh water section was not derived from remineralization of

350   fluvial organic matter in the river channel, but more likely from other sources (e.g., leaching of soil).

351   In the estuarine section, there may be some DON transformation occurred (Jiang et al., 2019), while

352   the leaching from soil process still cannot be eliminated (Fig. 8). For particulate phase, no relation

353   can be found between nitrate and particulate OM composition (figure not shown).

354   The atomic DOC/DON in Rajang averaged 50 in the river part, and increased to 140 (mean

355   value) in the estuary part (Fig. 7). Although the DOC/DON ratio was much higher when compared

356   to other tropical peatland river waters (around 10; Sjögersten et al., 2011), the ratio is comparable

357   with other peatland-draining rivers in Sarawak like the Lupar, Saruba and Maludan rivers (Müller

358   et al., 2015; Müller et al., 2016), which all enter the South China sea. The ratio is also within the

359   reported C/N ratio of peatland and leaves (Müller et al., 2016). For the Amazon river, the DOC

360   versus total nitrogen ratio ranges from 27 to 52 (Hedges et al., 1994). Given their reported total

361   nitrogen includes inorganic nitrogen, the DOC/DON ratio for the Amazon river would be even

362   higher. Under the background of such high C/N ratios (e.g., 50), transformation of DON to DIN in

363   the estuary further enhanced the high DOC/DON ratio (to 140), and hence a deficiency in terrestrial

364   organic nitrogen output is expected. We noted that dissolved inorganic nitrogen for Rajang is on the

365   order of 10 µM, comparable to DON (Jiang et al., 2019). Terrestrial nitrogen output is an important

source for coastal primary production (Jiang et al., 2019), but peatland-impacted rivers may have

relatively lower nitrogen input to the South China Sea when compared with their very high river

basin DOC yields (Baum et al., 2007). On one hand, logging and secondary growth has been found

to play a negative role in the nitrogen output efficiency of forest soils (Davidson et al., 2007). On

the other hand, disturbed tropical peatlands could release more DOC in comparison to an

undisturbed site (Moore et al., 2013) while the DOC/DON ratio may also decrease along with

disturbance of peatland (Kalbitz and Geyer, 2002). Given that secondary growth in river basin and

anthropogenic disturbance of peatland (e.g., drainage and conversion for oil palm) are both common

(Hooijer et al., 2015), changes of DOC/DON ratios in the Rajang are complex and further

assessment is needed in the future.

5. Summary and Conclusion

In August 2016 in the Rajang, we observed that dissolved OM composition (as D/L Glx ratio)

was conservatively diluted along with increasing DOC δ^{13}C, indicating that the sources of dissolved

OM have a very conservative impact on the OM composition. When D/L Glx ratio was plotted

against salinity (as is usually done for an estuarine OM behavior check in many studies), such linear

conservative dilution pattern disappeared (Figs. 4a&5a). This implies that the addition of DOC in

the estuary (peatland/mangrove) had an impact on dissolved OM composition, adding more bio-

degraded OM, and resulting in data above the theoretical dilution line (Figs. 4a&5a). For particulate

OM, though the data was variable, the overall decreasing GABA% or ratio along with salinity was

much clearer relative to that of dissolved OM (Figs. 4b&5b). Particulate D/L Glx ratio in the estuary

was usually lower when compared with that in the fresh water section (Figs. 6b&c), whereas for

dissolved OM, the majority of the samples in the estuary had a D/L Glx ratio similar to that in the fresh water (Fig. 6a). The difference in OM composition between fresh water and estuarine section suggests that dissolved OM became more degraded while particulate OM became less degraded in the estuary.

The Rajang is characterized by DOC/DON ratios of 50 in the fresh water section, and the further loss of DON in the estuary increased the ratio to 140. Peatland draining and logging/secondary growth are reported to have conflicting impacts on carbon and nitrogen cycling (Davidson et al., 2007; Moore et al., 2013), which may increase fluvial DOC and limit basin nitrogen output, resulting in even larger DOC/DON. Mismatch in carbon and nitrogen loss from tropical rivers due to anthropogenic activities plays a role in material cycle in both land and marine systems, enhancing the tropical river as a direct carbon source to atmosphere while for nitrogen change and its further feedback on carbon cycle needs further monitoring and assessment.

At last, this work is based on a dry season investigation (August). Though the seasonality for Rajang OM may be moderate (Martin et al., 2018), for biomarkers like amino acids enantiomers further investigation in the wet season is needed.

Acknowledgements

We thank captain and crew of the boat, as well as other colleagues on board during the field work. We thank colleagues and students in both Swinburne University of Technology (Sarawak Campus) and in State Key Lab of Estuarine and Coastal Research/East China Normal University. We thank Aazani Mujahid in University Malaysia Sarawak for her help and hospitality during our stay in Malaysia. This work is funded by the National Key Research and Development Program of

China (2018YFD0900702), MOHE FRGS 15 Grant (FRGS/1/2015/WAB08/SWIN/02/1) in

Malaysia, ARC Linkage Grant LP150100519 in Australia, a SKLEC Open Research Fund (SKLEC-

KF201610) and '111' project in SKLEC/ECNU from the Ministry of Education of China and State

Administration of Foreign Experts Affaires of China.

References

Amon, R. M. W., Fitznar, H. P., and Benner, R.: Linkages among the bioreactivity, chemical composition, and diagenetic state of marine dissolved organic matter, Limnology and Oceanography, 46, 287-297, 2001.

Baum, A., Rixen, T., and Samiaji, J.: Relevance of peat draining rivers in central Sumatra for the riverine input of dissolved organic carbon into the ocean, Estuarine, Coastal and Shelf Science, 73, 563-570, 2007.

Bianchi, T. S.: The role of terrestrially derived organic carbon in the coastal ocean: A changing paradigm and the priming effect, Proceedings of the National Academy of Sciences, 108, 19473-19481, 2011.

Bianchi, T. S. and Bauer, J. E.: Particulate Organic Carbon Cycling and Transformation. In: Treatise on Estuarine and Coastal Science, Editors-in-Chief: Eric, W. and Donald, M. (Eds.), Academic Press, Waltham, 2011.

Cifuentes, L. A., Coffin, R. B., Solorzano, L., Cardenas, W., Espinoza, J., and Twilley, R. R.: Isotopic and Elemental Variations of Carbon and Nitrogen in a Mangrove Estuary   Estuarine Coastal and Shelf Science, 43, 781-800, 1996.

Cloern, J. E., Foster, S. Q., and Kleckner, A. E.: Phytoplankton primary production in the world's estuarine-coastal ecosystems, Biogeosciences, 11, 2477-2501, 2014.

Dauwe, B. and Middelburg, J. J.: Amino acids and hexosamines as indicators of organic matter degradation state in North Sea sediments, Limnology and Oceanography, 43, 782-798, 1998.

Davidson, E. A., de Carvalho, C. J. R., Figueira, A. M., Ishida, F. Y., Ometto, J. P. H. B., Nardoto, G. B., Saba, R. T., Hayashi, S. N., Leal, E. C., Vieira, I. C. G., and Martinelli, L. A.: Recuperation of nitrogen cycling in Amazonian forests following agricultural abandonment, Nature, 447, 995-998, 2007.

Davis, J., Kaiser, K., and Benner, R.: Amino acid and amino sugar yields and compositions as indicators of dissolved organic matter diagenesis, Organic Geochemistry, 40, 343-352, 2009.

Dittmar, T., Fitznar, H. P., and Kattner, G.: Origin and biogeochemical cycling of organic nitrogen in the eastern Arctic Ocean as evident from D- and L-amino acids, Geochimica et Cosmochimica Acta, 65, 4103-4114, 2001a.

Dittmar, T., Lara, R. J., and Kattner, G.: River or mangrove? Tracing major organic matter sources in tropical Brazilian coastal waters, Marine Chemistry, 73, 253-271, 2001b.

Fitznar, H. P., Lobbes, J. M., and Kattner, G.: Determination of enantiomeric amino acids with high-performance liquid chromatography and pre-column derivatisation with o-phthaldialdehyde and N-isobutyrylcysteine in seawater and fossil samples (mollusks), Journal of Chromatography A, 832, 123-132, 1999.

Gandois, L., Teisserenc, R., Cobb, A. R., Chieng, H. I., Lim, L. B. L., Kamariah, A. S., Hoyt, A., and Harvey, C. F.: Origin, composition, and transformation of dissolved organic matter in tropical peatlands, Geochimica et Cosmochimica Acta, 137, 35-47, 2014.

Hedges, J. I., Cowie, G. L., Richey, J. E., Quay, P. D., Benner, R., Mike, S., and Forsberg, B. R.: Origins and processing of organic matter in the Amazon River as indicated by carbohydrates and amino acids, Limnology and Oceanography, 39, 743-761, 1994.

Hedges, J. I. and Man, D. C.: The characterization of plant tissues by their lignin oxidation products, Geochimica et Cosmochimica Acta, 43, 1803-1807, 1979.

Hernes, P. J., Robinson, A. C., and Aufdenkampe, A. K.: Fractionation of lignin during leaching and sorption and implications for organic matter "freshness", Geophysical Research Letters, 34, 2007.

Hooijer, A., Vernimmen, R., Visser, M., and Mawdsley, N.: Flooding projections from elevation and subsidence models for oil palm plantations in the Rajang delta peatlands, Sarawak, Malaysia, Deltares report 1207384, 76 pp., 2015.

Huang, T. H., Chen, C. T. A., Tseng, H. C., Lou, J. Y., Wang, S. L., Yang, L., Kandasamy, S., Gao, X., Wang, J. T., Aldrian, E., Jacinto, G. S., Anshari, G. Z., Sompongchaiyakul, P., and Wang, B. J.: Riverine carbon fluxes to the South China Sea, Journal of Geophysical Research: Biogeosciences, 122, 1239-1259, 2017.

Jennerjahn, T. C., Ittekkot, V., Klöpper, S., Adi, S., Purwo Nugroho, S., Sudiana, N., Yusmal, A., Prihartanto, and Gaye-Haake, B.: Biogeochemistry of a tropical river affected by human activities in its catchment: Brantas River estuary and coastal waters of Madura Strait, Java, Indonesia, Estuarine, Coastal and Shelf Science, 60, 503-514, 2004.

Jiang, S., Müller, M., Jin, J., Wu, Y., Zhu, K., Zhang, G., Mujahid, A., Rixen, T., Muhamad, M. F., Sia, E. S. A., Jang, F. H. A., and Zhang, J.: Dissolved inorganic nitrogen in a tropical estuary at Malaysia: transport and transformation, Biogeosciences Discuss., 2019, 1-27, 2019.

Kaiser, K. and Benner, R.: Biochemical composition and size distribution of organic matter at the Pacific and Atlantic time-series stations, Marine Chemistry, 113, 63-77, 2009.

Kaiser, K. and Benner, R.: Hydrolysis-induced racemization of amino acids, Limnology and Oceanography: Methods, 3, 318-325, 2005.

Kalbitz, K. and Geyer, S.: Different effects of peat degradation on dissolved organic carbon and nitrogen, Organic Geochemistry, 33, 319-326, 2002.

Kimber, R. W. L., Nannipieri, P., and Ceccanti, B.: The degree of racemization of amino acids released by hydrolysis of humic-protein complexes: Implications for age assessment, Soil Biology and Biochemistry, 22, 181-185, 1990.

Lamade, E., Setiyo, I. E., Girard, S., and Ghashghaie, J.: Changes in 13C/12C of oil palm leaves to understand carbon use during their passage from heterotrophy to autotrophy, Rapid Communications in Mass Spectrometry, 23, 2586-2596, 2009.

Lamb, A. L., Wilson, G. P., and Leng, M. J.: A review of coastal palaeoclimate and relative sea-level reconstructions using δ13C and C/N ratios in organic material, Earth-Science Reviews, 75, 29-57, 2006.

Martin, P., Cherukuru, N., Tan, A. S. Y., Sanwlani, N., Mujahid, A., and Müller, M.: Distribution and cycling of terrigenous dissolved organic carbon in peatland-draining rivers and coastal waters of Sarawak, Borneo, Biogeosciences, 15, 6847-6865, 2018.

Mayorga, E., Aufdenkampe, A. K., Masiello, C. A., Krusche, A. V., Hedges, J. I., Quay, P. D., Richey, J. E., and Brown, T. A.: Young organic matter as a source of carbon dioxide outgassing from Amazonian rivers, Nature, 436, 538-541, 2005.

Moore, S., Evans, C. D., Page, S. E., Garnett, M. H., Jones, T. G., Freeman, C., Hooijer, A., Wiltshire, A. J., Limin, S. H., and Gauci, V.: Deep instability of deforested tropical peatlands revealed by fluvial organic carbon fluxes, Nature, 493, 660, 2013.

494 Müller-Dum, D., Warneke, T., Rixen, T., Müller, M., Baum, A., Christodoulou, A., Oakes, J., Eyre, B.
495 D., and Notholt, J.: Impact of peatlands on carbon dioxide (CO2) emissions from the Rajang River and
496 Estuary, Malaysia, Biogeosciences, 16, 17-32, 2019.

497 Müller, D., Warneke, T., Rixen, T., Müller, M., Jamahari, S., Denis, N., Mujahid, A., and Notholt, J.:
498 Lateral carbon fluxes and CO_2 outgassing from a tropical peat-draining river,
499 Biogeosciences, 12, 5967-5979, 2015.

500 Müller, D., Warneke, T., Rixen, T., Müller, M., Mujahid, A., Bange, H. W., and Notholt, J.: Fate of
501 terrestrial organic carbon and associated CO2 and CO emissions from two Southeast Asian estuaries,
502 Biogeosciences, 13, 691-705, 2016.

503 Raymond, P. A. and Bauer, J. E.: Use of 14C and 13C natural abundances for evaluating riverine,
504 estuarine, and coastal DOC and POC sources and cycling: a review and synthesis, Organic Geochemistry,
505 32, 469-485, 2001.

506 Schleifer, K. H. and Kandler, O.: Peptidoglycan types of bacterial cell walls and their taxonomic
507 implications, Bacteriological Reviews, 36, 407-477, 1972.

508 Schroeder, R. A. and Bada, J. L.: A review of the geochemical applications of the amino acid racemization
509 reaction, Earth-Science Reviews, 12, 347-391, 1976.

510 Sjögersten, S., Cheesman, A. W., Lopez, O., and Turner, B. L.: Biogeochemical processes along a nutrient
511 gradient in a tropical ombrotrophic peatland, Biogeochemistry, 104, 147-163, 2011.

512 Vollmer, W., Blanot, D., and de Pedro, M.: Peptidoglycan structure and architecture, FEMS Microbiology
513 Review, 32, 149-167, 2008.

514 Wu, Y., Zhu, K., Zhang, J., Müller, M., Jiang, S., Mujahid, A., Muhamad, M. F., and Sia, E. S. A.:
515 Distribution and degradation of terrestrial organic matter in the sediments of peat-draining rivers,
516 Sarawak, Malaysian Borneo, Biogeosciences Discuss., 2019, 1-37, 2019.

517 Zhang, C. L., Dang, H. Y., Azam, F., Benner, R., Legendre, L., Passow, U., Polimene, L., Robinson, C.,
518 Suttle, C. A., and Jiao, N. Z.: Evolving paradigms in biological carbon cycling in the ocean, National
519 Science Review, 5, 481-499, 2018.

520 Zhu, Z. Y., Wu, Y., Zhang, J., Dittmar, T., Li, Y., Shao, L., and Ji, Q.: Can primary production contribute
521 non-labile organic matter in the sea: Amino acid enantiomers along the coast south of the Changjiang
522 Estuary in May, Journal of Marine Systems, 129, 343-349, 2014.

523 Zhu, Z. Y., Zhang, J., Wu, Y., and Lin, J.: Bulk particulate organic carbon in the East China Sea: Tidal
524 influence and bottom transport, Progress in Oceanography, 69, 37-60, 2006.

525
526

527   Table 1. Measured amino acids (the L- and D- enantiomers are not listed) and all abbreviations in
528   this study. Note that glycine has no enantiomer.

name	abbreviations
organic matter	OM
dissolved organic carbon	DOC
dissolved organic nitrogen	DON
total suspended matter	TSM
amino acid	AA
total hydrolysable dissolved amino acids	TDAA
total hydrolysable particulate amino acids	TPAA
Alanine	Ala
Arginine	Arg
Asparagine Aspartic acid	Asx
Glutamine Glutamic acid	Glx
Glycine	Gly
Isoleucine	Ile
Leucine	Leu
Lysine	Lys
Methionine	Met
Phenylalanine	Phe
Serine	Ser
Threonine	Thr
Tryptophan	Trp
Tyrosine	Tyr
Valine	Val
γ - aminobutyric acid	GABA

529
530

531 Table 2. TSM, DOC, POC and stable carbon isotopes in the freshwater and estuary of the Rajang
532 (mean (min-max)).
533

	unit	Fresh water	Estuary
TSM	mg/L	61 (22 - 126)	73 (25 - 161)
DOC	μM	337 (217 - 658)	345 (214 - 587)
DOC δ^{13}C	‰	−26.7 (−27.7 - −25.0)	−26.1 (−28.7 - −20.1)
POC	μM	86 (46 - 125)	64 (22 - 153)
	%	1.9 (1.2 - 2.5)	1.0 (0.6 - 1.9)
POC δ^{13}C	‰	−30.1 (−31.1 - −29.4)	−26.7 (−30.1 - −23.8)

534
535
536
537
538 Table 3 The Rajang AAs result (mean (min-max)) in August 2016 (*total D/TDAA means total D
539 form AA versus TDAA, the same for total D/TPAA)
540

		unit	Fresh water	Estuary
dissolved	TDAA	nM	317 (131 - 486)	523 (212 - 2320)
	TDAA carbon yield	%	0.40 (0.08 - 0.65)	0.38 (0.29 - 0.53)
	TDAA nitrogen yield	%	4.8 (1.3 - 15)	11 (5.4 - 18)
	GABA	%	2.0 (1.3 - 4.1)	1.3 (0.15 - 1.9)
	total D/total TDAA*	%	12 (8 - 15)	12 (3 - 14)
	D/L Glx		0.35 (0.16 - 0.57)	0.32 (0.07 - 0.42)
	D/L Asx		0.34 (0.23 - 0.48)	0.34 (0.08 - 0.42)
particulate	TPAA	μM	2.5 (1.4 - 3.6)	2.0 (1.1 - 3.7)
	TPAA carbon yield	%	14 (9.5 - 19)	17 (11 - 24)
	TPAA nitrogen yield	%	66 (36 - 82)	62 (30 - 100)
	GABA%	%	0.7 (0.6 - 0.9)	0.4 (0.2 - 0.8)
	total D/total TPAA*	%	4.4 (3.6 - 5.2)	3.3 (2.4 - 5.0)
	D/L Glx		0.09 (0.08 - 0.10)	0.06 (0.04 - 0.08)
	D/L Asx		0.04 (0.03 - 0.05)	0.05 (0.03 - 0.11)

541
542

Figure caption

Figure 1. Study area and sampling stations. a) Location of Sarawak, Malaysia; and b) the Rajang with its estuary/river mouth background shown. Samples upstream of S5 showed 0 salinity while downstream of S5 showed salinity >0. Hence here from S5 to S10 is regarded as the fresh water section (red triangles), and downstream of S5 is regarded as the estuarine section (blue triangles). Note that salinity of samples at S15, S17, S18, S19 was also 0 during our sampling.

Figure 2. Distribution pattern of (a) TSM, (b) DOC and (c) POC along with salinity in the Rajang. The fresh water dot stands for all samples with S = 0 and the error bar corresponds to the standard deviation. The marine dot is S1.

Figure 3. Distribution pattern of (a) DOC δ^{13}C and (b) POC δ^{13}C along with conductivity/salinity in the Rajang. The legend indicates the branches that the samples were from and marine corresponds to S1 station.

Figure 4. GABA% distribution pattern from fresh water to estuary in the Rajang: a) dissolved and b) particulate. Note the different x-axis scales between plot a and b. The dashed line indicates the linear mixing line between fresh and marine endmembers. For the fresh water endmember (brown triangle), it is calculated as the means of all fresh samples (S = 0), and the marine endmember (purple diamond) is calculated as the means of all offshore samples with salinity >30. The error bar indicates the standard deviation.

Figure 5. Same as figure 4, but for D/L-Glx.

Figure 6. D/L ratio of AAs (as Glx) plotted against a) DOC δ^{13}C b) POC δ^{13}C, and c) PN δ^{15}N.

Figure 7. DOC/DON ratio distribution pattern along with salinity in the Rajang. For fresh water and estuary, the mean DOC/DON value was 50 and 140, respectively. DON is from Jiang et al., (2019)

Figure 8. Dissolved OM composition (a: D/L Glx, b: GABA%) and its relation with nitrate. Nitrate is derived from Jiang et al., (2019).

572

573

574 Figure 1.

575

576

577

578

579

580

581   Figure 2.

582

583

584

585   Figure 3.

586

587

588

589

590

591   Figure 4.

592

593

594

595   Figure 5.

596

597

601   Figure 6.

602

603

604

605

606   Figure 7.

607

608

609
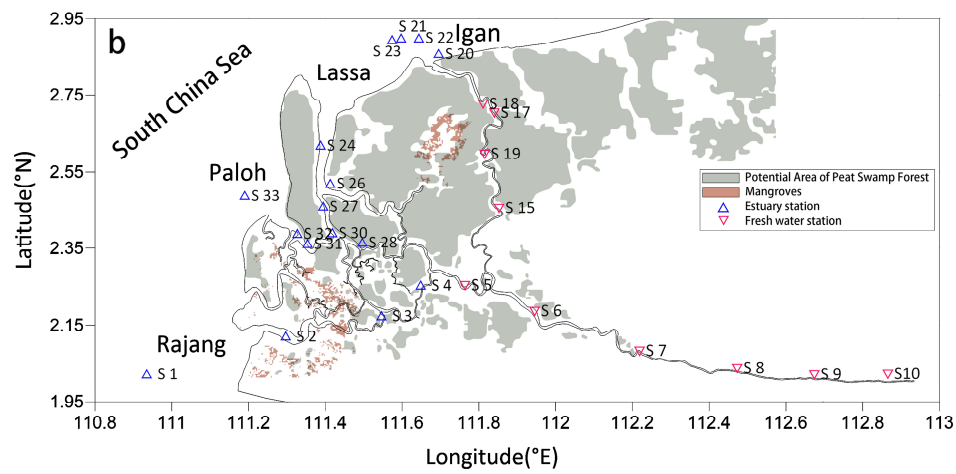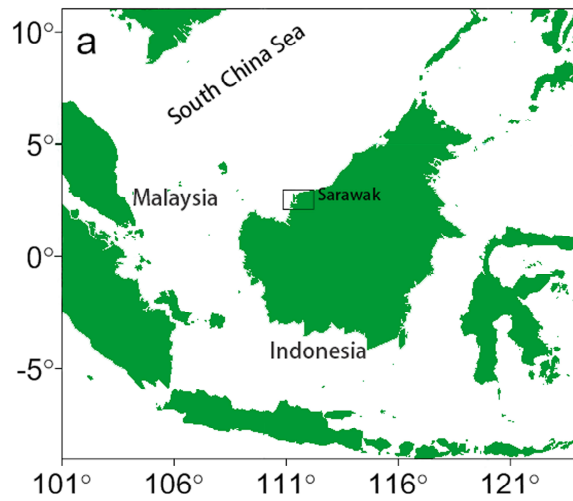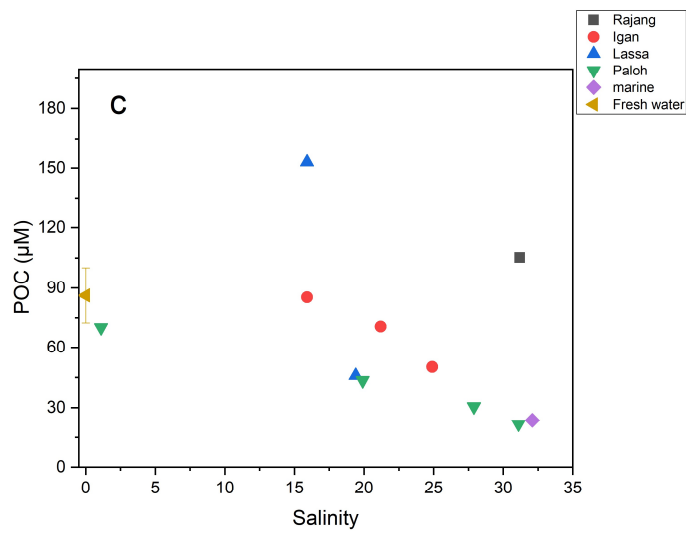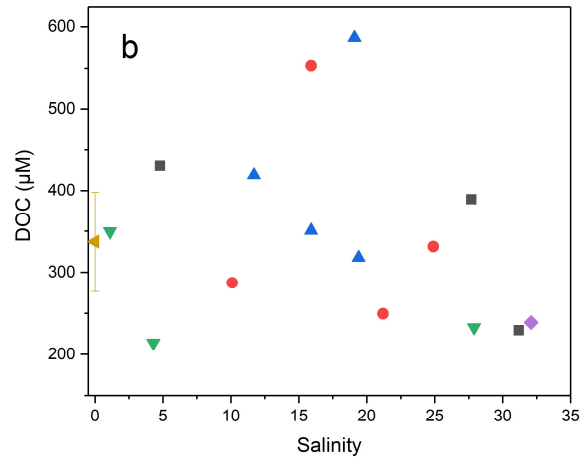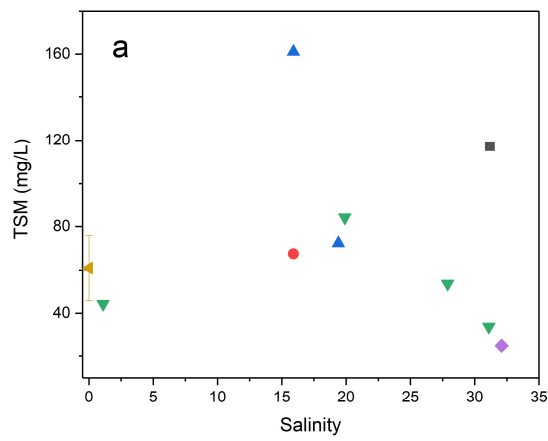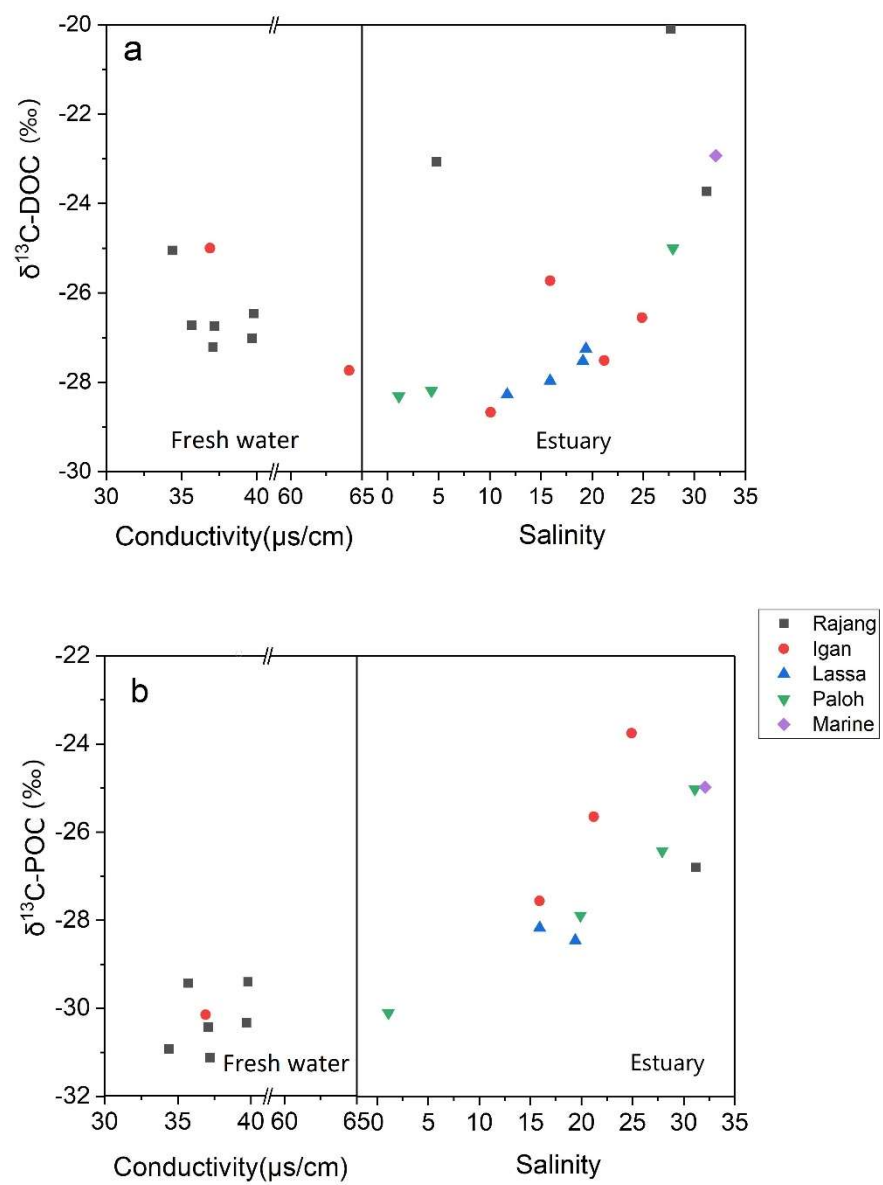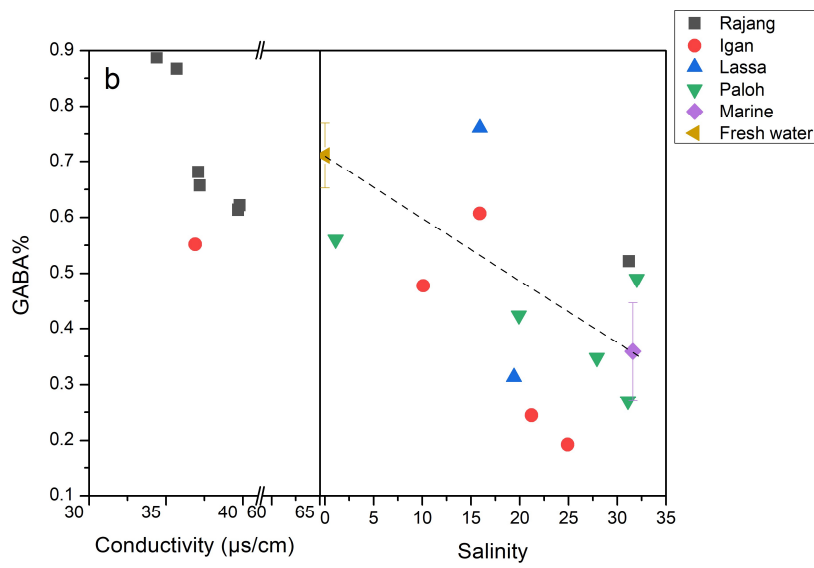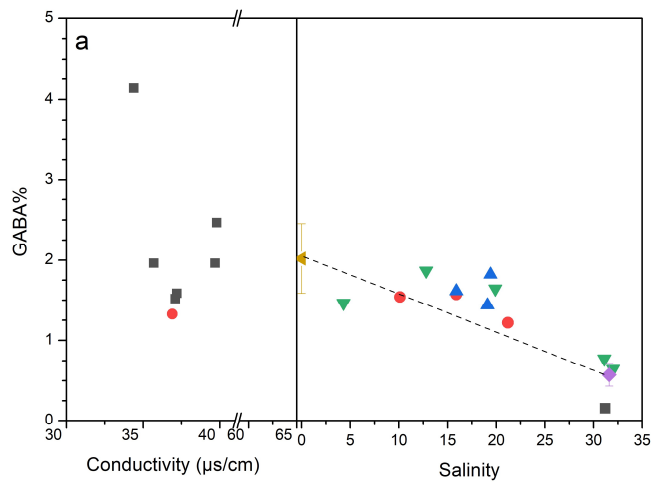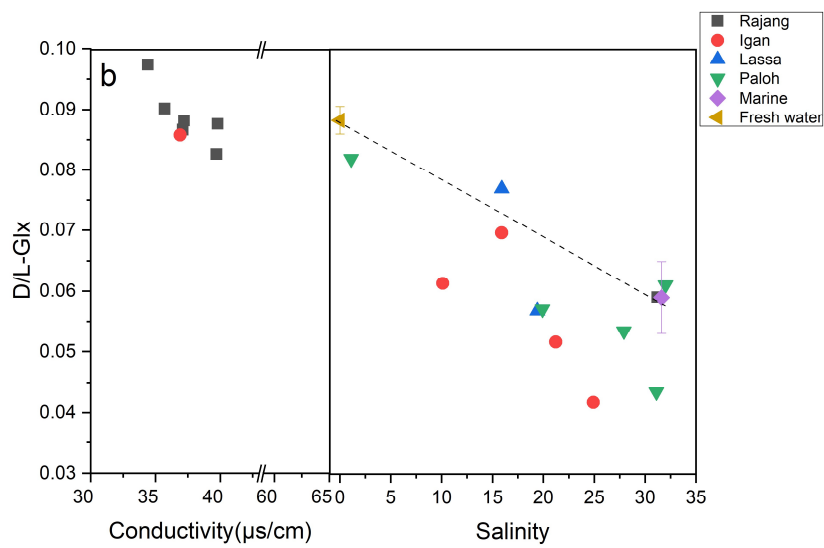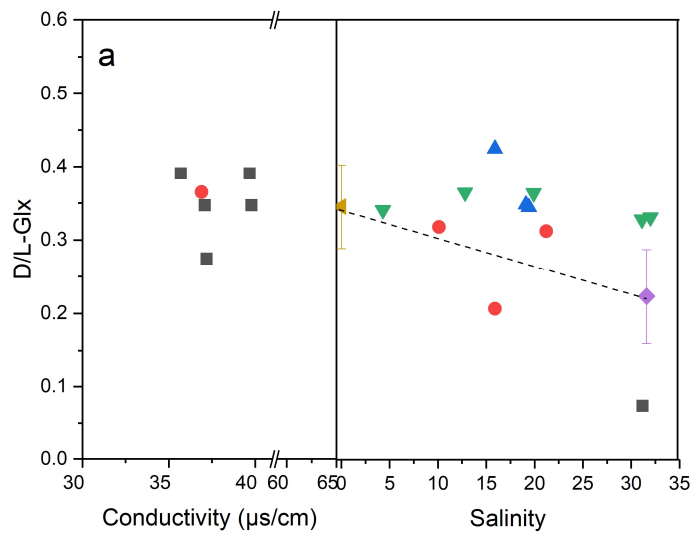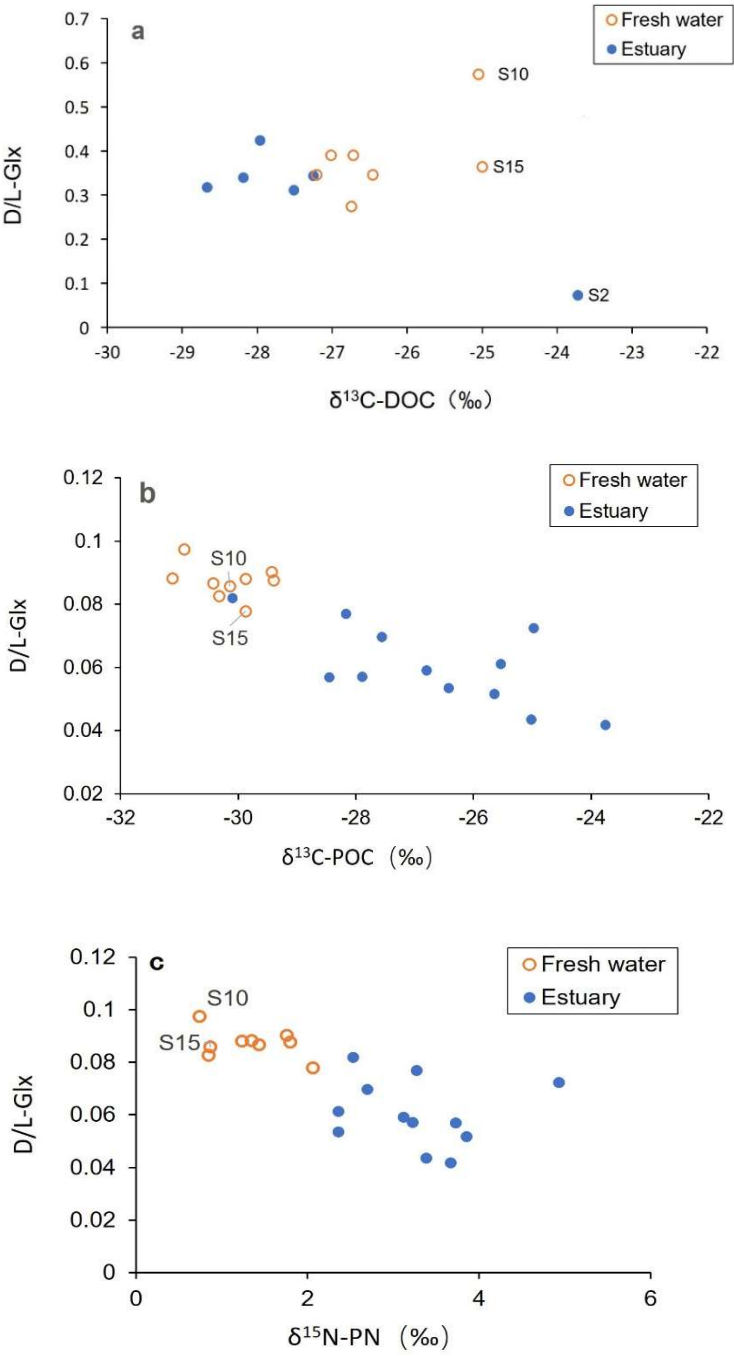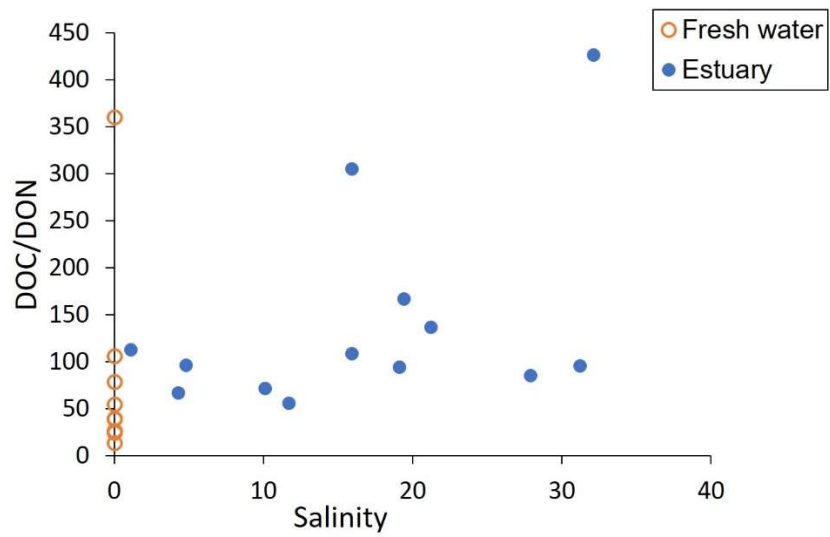
610

611

612

613

614   Figure 8.